Human Molecular Genetics, 2011, Vol. 20, No. 5 **905–916**
doi:10.1093/hmg/ddq529
Advance Access published on December 7, 2010

Notch inhibition by the ligand Delta-Like 3 defines the mechanism of abnormal vertebral segmentation in spondylocostal dysostosis

Gavin Chapman[1,2,*], Duncan B. Sparrow[1,2], Elisabeth Kremmer[3] and Sally L. Dunwoodie[1,2]

[1]Developmental Biology Division, Victor Chang Cardiac Research Institute, Sydney, Australia, [2]St Vincent's Clinical School, University of New South Wales, Sydney, Australia and [3]Institut für Molekulare Immunologie, Helmholtz Zentrum München, Marchioninistraße 25, 81377 München, Germany

Received September 7, 2010; Revised November 11, 2010; Accepted December 1, 2010

Mutations in the *DELTA-LIKE 3* (*DLL3*) gene cause the congenital abnormal vertebral segmentation syndrome, spondylocostal dysostosis (SCD). DLL3 is a divergent member of the DSL family of Notch ligands that does not activate signalling in adjacent cells, but instead inhibits signalling when expressed in the same cell as the Notch receptor. Targeted deletion of *Dll3* in the mouse causes a developmental defect in somite segmentation, and consequently vertebral formation is severely disrupted, closely resembling human SCD. In contrast to the canonical Notch signalling pathway, very little is known about the mechanism of *cis*-inhibition by DSL ligands. Here, we report that Dll3 is not presented on the surface of presomitic mesoderm (PSM) cells *in vivo*, but instead interacts with Notch1 in the late endocytic compartment. This suggests for the first time a mechanism for Dll3-mediated *cis*-inhibition of Notch signalling, with Dll3 targeting newly synthesized Notch1 for lysosomal degradation prior to post-translational processing and cell surface presentation of the receptor. An inhibitory role for Dll3 *in vivo* is further supported by the juxtaposition of Dll3 protein and Notch1 signalling in the PSM. Defining a mechanism for *cis*-inhibition of Notch signalling by Dll3 not only contributes greatly to our understanding of this ligand's function during the formation of the vertebral column, but also provides a paradigm for understanding how other ligands of Notch *cis*-inhibit signalling.

INTRODUCTION

Abnormal vertebral segmentation (AVS) in humans is a common congenital abnormality (2 per 1000 births) that results in uneven or fused vertebrae. The majority of AVS cases are mild and involve only a few vertebrae. This is termed congenital scoliosis and results in an abnormal lateral curvature of the vertebral column. Ten percent of cases are classified as severe in that they have multiple contiguous vertebral malformations. Spondylocostal dysostosis (SCD) is the best-studied example of the latter group and is characterized by rib fusions, rib deletions, hemivertebrae and loss of vertebrae, causing truncal shortening. Mutations in four genes involved in the Notch signalling pathway [*DELTA-LIKE 3* (*DLL3*), *MESP2*, *LFNG* and *HES7*] account for ~30% of SCD cases (1–4). Mutation of *DLL3* is the most common cause of SCD and yet the role of DLL3 in Notch signalling and in vertebral column formation is not understood.

Vertebrae and ribs derive from somites. These structures are formed by segmentation of the presomitic mesoderm (PSM) in a reiterative process that occurs every 120 min in the mouse (reviewed in 5) and is estimated to occur every 4–6 h in humans (6,7). This process is thought to be controlled at the molecular level by the finely balanced interaction of two signalling processes: the 'clock' and the 'wavefront' (reviewed in 8). The 'wavefront' is thought to be generated by two opposing gradients of signalling (Fgf8 from the caudal PSM and retinoic acid from the rostral PSM). The 'clock' is characterized by a series of genes whose expression oscillates with a period equal to the time it takes to make a single somite. There are many genes with such expression (9), but an important subset are direct transcriptional targets of Notch

*To whom correspondence should be addressed at: Developmental Biology Division, Victor Chang Cardiac Research Institute, 405 Liverpool Street, Darlinghurst, NSW 2010, Sydney, Australia. Tel: +61 292958630; Fax: +61 292958668; Email: g.chapman@victorchang.edu.au

© *The Author 2010. Published by Oxford University Press. All rights reserved.*
For Permissions, please email: journals.permissions@oup.com

signalling, such as *Hes1*, *Hes7*, *Hey1* and *2*, *Lfng* and *Nrarp* (10–14). It is likely that the expression of these genes is directly controlled by the induction of Notch1 receptor signalling, which also occurs in a cyclical manner (15,16). Notch signalling itself is not thought to initiate this cycling process, rather it is likely to maintain a previously initiated oscillation by synchronizing gene expression in adjacent PSM cells (17,18). Notch signalling also has two other key roles in the process of somitogenesis: it is required for somite boundary formation and for the establishment of the anterior–posterior polarity of somites (15,18–21). Like individuals with SCD, mice null for *Dll3*, *Mesp2*, *Lfng* and *Hes7* all exhibit extensive malformation of vertebra. In these embryos, the anterior–posterior polarity of somites is disrupted, and in the case of *Dll3*, *Lfng* and *Hes7* embryos, a loss of cyclic Notch1 signalling occurs in the PSM (22–24).

Signalling via the Notch receptors is widely conserved and utilized in metazoans for communication between cells in contact. The Notch receptors (Notch1–4 in mammals) are synthesized as a single polypeptide which then undergoes a series of post-translation modifications: fucosylation of EGF-like repeats in the endoplasmic reticulum (ER); glycosylation of *O*-fucose by Fringe family enzymes in the *cis*-Golgi; and cleavage (S1) by a furin-like convertase in the *trans*-Golgi network (TGN) to produce a covalently linked heterodimer (25–29). Once modified and processed, the receptor is presented on the cell surface, where it can interact with DSL ligands of the Delta and Serrate families [Delta-Like 1 (Dll1), Delta-Like 4 (Dll4), Jagged1 and Jagged2 in mammals] expressed on the surface of neighbouring cells. Receptor–ligand interaction between cells (*in trans*) triggers canonical Notch signalling, which initiates with ligand endocytosis, causing receptor transendocytosis and extracellular domain shedding. This exposes the S2 cleavage site of the receptor, allowing ADAM10/17 cleavage (30,31). The remaining portion of Notch is a substrate for γ-secretase, causing S3 cleavage within the transmembrane domain and release of the intracellular domain (NICD) into the cytoplasm (30,32). NICD translocates to the nucleus, where it interacts with the transcription factor CSL, causing the release of co-repressors and recruitment of Maml and other coactivators, thereby activating transcription of Notch target genes (33–37).

The ability of a Notch1-expressing cell to respond to ligand activation *in trans* is in part controlled by the amount of receptor presented on the cell surface. This is not a static property of the responding cell, as presentation of the receptor at the cell surface is a dynamic process. In the absence of ligand *in trans*, a proportion of processed Notch1 is removed from the cell surface via the endocytic pathway and can then be either returned to the cell surface or directed to the lysosomal degradation pathway (38–40). The endocytic pathway is a major part of the protein transport and sorting system of the cell (reviewed in 41). Endocytosed proteins are carried by transport vesicles to early endosomes that act as a sorting station, returning some proteins to the cell surface via recycling endosomes, sending others to the TGN. The remaining proteins are held within the endosome, which then undergo maturation to form the late endosome. The late endosomes then undergo a series of fusion and fission cycles to form lysosomes, which are acidic organelles that degrade endocytosed proteins. Degradation of cargo begins in the late endosomes and continues in the lysosome. This pathway also interacts with the normal biosynthetic pathway of the cell. Newly translated proteins synthesized in the ER can be transported through the Golgi to the TGN, and from here directly to the late endosomes and lysosomes. Proteins following this pathway include those required for normal lysosomal function, as well as proteins targeted for degradation.

The pattern of Notch signalling is a product of activation and inhibition of the signalling pathway and these opposing influences can be mediated by DSL ligands of Notch. The mechanisms in place that control the relative activation and inhibition of Notch signalling are ill-defined. DSL ligands expressed on the surface of neighbouring cells activate Notch signalling *in trans*, but when expressed in the same cell as the Notch receptors (*in cis*), they inhibit signalling from ligand *in trans*. This phenomenon has been reported in *Drosophila* systems such as the imaginal disc, as well as in mammalian cell culture; however, the significance of *cis*-inhibition in mammals is not known, nor is the mechanism understood. There have been various reports showing that ligand/receptor complex formation *in cis* appears to block signalling *in trans* (42), or that *cis*-inhibition occurs inside the cell, or at the plasma membrane (42,43). The ability of DSL ligands to both activate and repress signalling makes it impossible to elucidate the relative impact of signalling activation versus inhibition and to define the means by which ligands *cis*-inhibit Notch signalling. We have taken advantage of the fact that Dll3 is unique among Notch ligands. Dll3 is a divergent DSL ligand that, when deleted in the mouse, causes a developmental defect in which vertebral formation is severely disrupted (22). We have found that Dll3 cannot compensate for the loss of Dll1 during somitogenesis, indicating that Dll3 functions differently from Dll1 (24). Indeed, recapitulation of Notch signalling *in vitro* via co-culture of ligand and receptor-expressing cells indicates that Dll3 cannot induce canonical Notch1 signalling (44), making it unique among the family of DSL ligands. Instead, Dll3 inhibits Notch1 signalling when expressed in the same cells as the receptor (*cis*-inhibition), the only function so far attributed to Dll3 (44). Dll3 interacts with Notch1, but only when the two proteins are expressed in the same cell (44). It is not clear how Dll3 inhibits Notch1 signalling *in cis*. It is also not certain where Dll3-mediated *cis*-inhibition occurs in the cell because different reports place Dll3 either in the Golgi apparatus or on the cell surface (24,44).

Here, we report that Dll3 interacts exclusively with the unprocessed full-length form of Notch1 and show that Dll3 is not present on the cell surface, instead it is intracellular and localizes to the *cis*-Golgi and cytoplasmic vesicles. In addition, co-localization of Dll3 and Notch1 occurs only in cytoplasmic vesicles that are likely to be late endosomes and lysosomes. In the PSM, co-localization of Dll3 and Notch1 is restricted to a somite-sized region, caudal to the forming somite (designated S-1) (45) and adjacent to regions of Notch1 signalling. In the absence of Dll3, Notch1 signalling is found in the rostral PSM only and it fails to become restricted in width to a few cells as it does in wild-type embryos. These observations for the first time suggest a mechanism for Dll3-mediated *cis*-inhibition of Notch signalling,

whereby Dll3 targets Notch1 for lysosomal degradation preventing Notch1 from undergoing post-translational processing that is necessary for cell surface presentation and activation. In the PSM, the degradation of Notch1 through interaction with Dll3 leads to the refinement of the Notch1 signalling domain in the PSM and hence regular positioning of the forming somite border.

RESULTS

Dll3 and Dll1 interact with unprocessed Notch1 *in cis*

DSL ligands such as Jagged1, Dll1 and Dll4 inhibit Notch signalling when expressed in the same cell as the receptor, in addition to activating Notch signalling *in trans* (reviewed in 46,47). The mechanism and subcellular location of *cis*-inhibition remain obscure. Unlike other DSL ligands, Dll3 cannot induce Notch signalling *in trans* (44), making it a useful protein to study *cis*-inhibition of Notch signalling without complications from *trans* effects. Previous studies indicate that Notch1 interacts with Dll1 or Dll3 when co-expressed in a human embryonic kidney cell line (HEK293T) (44); however, nothing more is known about the site or nature of this interaction. To further elucidate, we investigated the subcellular localization of Notch1 in the presence or absence of Dll1 or Dll3 to determine where in the cell they interact. For these experiments, we stably transfected the mouse myoblast cell line (C2C12) (48,49) with full-length Notch1 or with HA-tagged Dll3. C2C12 cells are of mesodermal origin and are prevented from undergoing differentiation by Notch signalling (50,51). Cells with and without Notch1 expression were transiently transfected with expression constructs encoding either Dll1 or Dll3 and stained to detect Dll3, Dll1 and/or Notch1. In the absence of Dll3 or Dll1, Notch1 was generally found either in large intracellular structures in transiently transfected cells or in smaller intracellular vesicles in stably transfected cells (Fig. 1A and B). However, in neither case did Notch1 co-localize with the *cis*-Golgi marker GM130. As previously reported, Dll3 is prominently expressed in the *cis*-Golgi, and to a lesser extent in cytoplasmic vesicles (Supplementary Material, Fig. S1A) (24). In the presence of Notch1, it was apparent that some Dll3-containing cytoplasmic vesicles also contained Notch1 (Fig. 1C). Dll1 was found at the cell surface, in scattered intracellular puncta and in a perinuclear region that overlaps with the *cis*-Golgi marker GM130 (Supplementary Material, Fig. S1B). In the presence of Notch1, Dll1 and Notch1 co-localized in the intracellular vesicles (Fig. 1D). Thus, Dll1 and Dll3 co-localize with Notch1 in intracellular vesicles when expressed in the same cell. Interestingly, when Notch1 was transfected into C2C12 cells stably expressing Dll3-HA, *cis*-Golgi localization of Dll3 was retained in cells where Notch1 was found in small intracellular vesicles (Fig. 1E) but was often lost in cells where Notch1 was found in large intracellular structures (Fig. 1F).

Notch1 is translated as a single polypeptide which then undergoes post-translational cleavage to produce a covalently linked heterodimer (27,28). The vast majority of cell-surface Notch1 is heterodimeric, and this form is required for robust ligand-dependent signalling (27,28,31,52,53). Interaction between DSL ligands and Notch1 *in cis* has been reported (42,44) (Supplementary Material, Fig. S1C). To determine which forms of Notch1 interact with Dll3 *in cis,* we immunoprecipitated Dll3 from transiently transfected C2C12 and HEK293 cells stably expressing Notch1. To avoid artefacts due to overexpression, we used a clonal cell line expressing Notch1 at a level approximately the same as that seen *in vivo*. In both cell types, only full-length Notch1 co-immunoprecipitated with Dll3, even though the lysates contained similar amounts of full-length and heterodimeric Notch1 (Fig. 1G, lanes 5 and 7), or an excess of heterodimeric Notch1 (Supplementary Material, Fig. S1D, lanes 2 and 4). To eliminate the possibility that the Notch1 heterodimer dissociates from Dll3 during the immunoprecipitation procedure, dithiobissuccinimidylpropionate (DSP) was used prior to immunoprecipitation to form stable crosslinks between the receptor and ligand. DSP treatment did not alter our results (data not shown). Consistent with data from the chick (42), both heterodimeric and full-length Notch1 co-precipitated with Dll1 when Notch1 and Dll1 are co-expressed in the same cell, demonstrating that heterodimeric Notch1 was capable of being co-immunoprecipitated under these conditions (Fig. 1G, lane 3). This interaction required the extracellular and transmembrane domains of Dll1 because the C-terminal fragment of Dll1 alone is unable to co-immunoprecipitate Notch1 (Supplementary Material, Fig. S1E). Together, these data indicate that both Dll1 and Dll3 interact with full-length Notch1 in a cell-autonomous manner. Moreover, the Notch1–Dll3 interaction occurs inside the cell because little or no full-length Notch1 makes it to the cell surface (28,52) (Supplementary Material, Fig. S1F).

Dll3 is not presented on the cell surface in the PSM of the embryo

The observation that Dll3 interacts with the unprocessed full-length form of Notch1 is consistent with our previous observations that Dll3 is localized to the Golgi apparatus and to unidentified cytoplasmic vesicles in the PSM cells of the mouse embryo, and that Dll3 is not found in significant amounts on the surface of cell lines transiently or stably transfected with Dll3 (24). However, another study has reported that overexpressing Dll3 leads to its detection on the surface of L cells (a mouse fibroblast cell line) (44). To resolve this issue, we examined the cell surface presentation of Dll3 *in vivo* by performing wholemount immunofluorescence on unfixed 9.5 dpc mouse embryos. Under these conditions, the cell membranes remain intact, antibody is unable to penetrate and hence immunoreactivity is limited to the extracellular domains of cell-surface proteins. In contrast, if the unfixed embryos are treated with Triton X-100, the cell membranes become permeable to the extent that antibody can pass freely into the cell. Freshly dissected 9.5 dpc embryos were cut in half along the neural tube and stained under non-permeabilized and Triton X-100-permeabilized conditions using antibodies against the N-terminal epitopes of Dll1 and Dll3 (24). In non-permeabilized embryos, these N-terminal epitopes will be detected only if the ligands are presented on the plasma membrane. Endogenous Dll1 was detected in the non-permeabilized PSM in a pattern characteristic of the

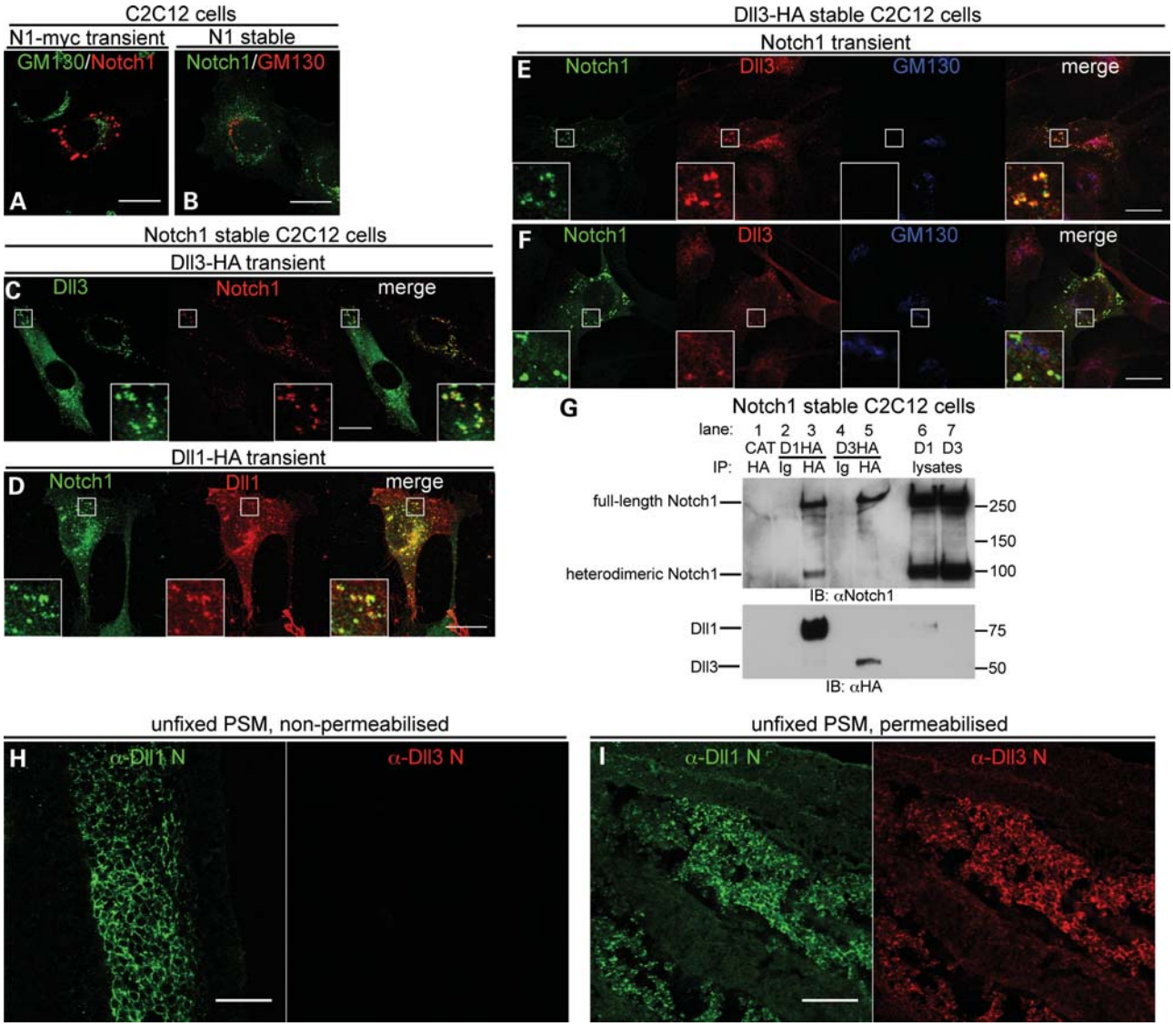

Figure 1. Dll1 and Dll3 interact with unprocessed Notch1 *in cis*. (**A** and **B**) Double staining of Notch1 and GM130 reactivity in C2C12 cells. (A) GM130 (αGM130, green) and Notch1 reactivity (αmyc, red) in C2C12 cells transiently transfected with myc-tagged Notch1. (B) Notch1 (αNotch1, green) and GM130 (αGM130, red) reactivity in C2C12 cells stably expressing Notch1. (**C**) Co-localization of Dll3 (αDll3, green) and Notch1 (αmyc, red) in Notch1 stable C2C12 cells transfected with Dll3-HA. (**D**) Notch1 (αNotch1, green) and Dll1 (αHA, red) co-localize in Notch1 stable C2C12 cells transfected with Dll1-HA. (**E** and **F**) Examples of Notch1-transfected Dll3HA stable C2C12 cells stained to detect Notch1 (αNotch1, green), Dll3 (αHA, red) and GM130 (αGM130, blue). (**G**) Dll1 and Dll3 interact with unprocessed Notch1. Notch1 stable C2C12 cells were transiently transfected with plasmids encoding Dll1HA (D1HA), Dll3HA (D3HA) or CAT as a control. Proteins were immunoprecipitated with either mouse αHA (HA, lanes 1, 3 and 5) or non-specific mouse IgG (Ig, lanes 2 and 4) and immunoblotted to detect Notch1 (intracellular domain epitope, C20) and HA reactivity. Full-length (unprocessed) Notch1 precipitates with Dll1HA (lane 3) and Dll3HA (lane 5) using anti-HA. Dll1HA also precipitates processed Notch1 TMIC of the heterodimer whereas Dll3 does not. (H–I) Dll3 is not presented on the cell surface *in vivo*. Wholemount immunofluorescence on fresh dissected (unfixed) non-permeabilized (**H**) or Triton-X-permeabilized 9.5 dpc mouse embryos (**I**) using antibodies against the N-terminal epitopes of Dll1 (green) and Dll3 (red). Scale bars represent 20 μm in (A–F) and 50 μm in (H–I).

plasma membrane, indicative of cell surface presentation (Fig. 1H). In contrast, endogenous Dll3 was never detected in the non-permeabilized PSM (Fig. 1H), consistent with observations in non-permeabilized Dll3HA-transfected C2C12 cells using the same approach (Supplementary Material, Fig. S1G–I). As a positive control, the Dll3 antibody was used to stain permeabilized tissue, and in this case was able to detect punctate Dll3 staining (Fig. 1I) consistent with our previous studies (24). Likewise, endogenous Dll1 intracellular expression was detectable in permeabilized tissue (Fig. 1I). We conclude that endogenous Dll3 is not present on the cell surface of PSM cells *in vivo*, whereas endogenous Dll1 is present on the cell surface.

Notch1 and Dll3 co-localize in vesicles of the late endocytic compartment

One possible mode of action of ligand-mediated *cis*-inhibition of Notch1 signalling is that ligand acts to trigger degradation of full-length Notch1. Since Dll3 is predominantly present in

the *cis*-Golgi (24), we examined the major pathway of protein degradation from the Golgi, which is via the late endosome/lysosome pathway. Such degradation prior to S1 processing would prevent trafficking of newly synthesized Notch1 to the cell membrane, and thereby reduce that cell's response to adjacent DSL ligand-expressing cells. To determine whether Dll3 protein is associated with this pathway, we co-stained C2C12 cells stably expressing Dll3 with markers of the different stages of the endocytic pathway. In addition to the previously described Golgi staining, Dll3 co-localized with the lysosomal markers Lamp1 and Lamp2 (Fig. 2A, not shown), the late endosome markers Vti1b, Rab7-GFP and Rab9-GFP (Fig. 2B; Supplementary Material, Fig. S1J and K) but not the early endosome marker EEA1 (Supplementary Material, Fig. S1L). Dll1 was also found in Lamp1-positive intracellular vesicles in transiently transfected C2C12 cells (Fig. 2C). Importantly, we confirmed that Dll3 was present in these organelles *in vivo* by wholemount staining 9.5 dpc mouse embryos with Dll3 and Lamp1 antibodies, detecting Dll3 in some, but not all, Lamp1-positive vesicles in the PSM (Fig. 2D). We conclude that Dll3 is found in the late endocytic compartment (late endosome/lysosome) in cultured cells and in embryos, in addition to its previously documented *cis*-Golgi localization.

In C2C12 cells, transfected Notch1 was not found in the *cis*-Golgi (Fig. 1A and B). To confirm that these results were representative of the situation *in vivo*, we examined Notch1 and GM130 localization in 9.5 dpc mouse embryos by wholemount immunofluorescence, observing that Notch1 is not localized to the *cis*-Golgi in the PSM *in vivo* (Fig. 2E). Notch1-positive vesicles in stably transfected C2C12 cells also contained Lamp1, Lamp2, Vti1b, Rab7-GFP and Rab9-GFP, indicating that Notch1, like Dll3, is found in late endosomes and lysosomes (Fig. 2F and G; data not shown; Supplementary Material, Fig. S2A and B). We did not detect Notch1 in caveolae, nor multivesicular bodies as marked by anti-Caveolin and anti-Hrs antibodies, respectively (Supplementary Material, Fig. S2C and D). Moreover, in live C2C12 cells, a Notch1–GFP fusion was often found in vesicles that also contained Lysotracker Red, a dye that selectively accumulates in acidic organelles such as lysosomes (Supplementary Material, Fig. S2E). Critically, Notch1 co-localized with Lamp1 in the rostral PSM, defined as the forming and prospective somites (S0 and S-1) (45), demonstrating that Notch1 is found in the late endocytic/lysosomal compartment *in vivo* (Fig. 2H).

To provide more evidence that the vesicles containing both Dll3 and Notch1 *in vivo* were indeed lysosomal in origin, we examined Dll3, Notch1 and Lamp1 expression in 9.5 dpc embryos by wholemount immunofluorescence. Intense Notch1 expression was restricted to Lamp1-positive vesicles, which also contained Dll3 (Fig. 2I). In addition, Dll3 was also found in larger puncta, presumably Golgi. Histogram and co-localization threshold images confirm the co-localization between Dll3, Notch1 and Lamp1 (Supplementary Material, Fig. S2F–J), with ~86% of Dll3/Notch double-positive locations also staining for Lamp1. Hence, in the rostral PSM, where their expression overlaps, Notch1 and Dll3 co-localize in the late endocytic compartment, implying that they are undergoing degradation.

Subcellular co-localization of Dll3 and Notch1 occurs in the rostral PSM

Given that Dll3 and Notch1 appear to co-localize in the rostral PSM, we sought to define the spatial pattern of Dll3 and Notch1 protein expression *in vivo*. We confirmed our previous observations that Dll3 is found throughout the PSM in a punctate pattern characteristic of the Golgi (Fig. 3A–C) (24). However, Dll3 expression was somewhat diminished in the rostral PSM. To define the rostral limit of high Dll3 expression, 9.5 dpc embryos were co-stained with anti-Dll3 and anti-EphA4, which is expressed in the prospective (S-1), forming (S0) and, to a lesser degree, in the nascent somite (S1) (54). Dll3 was expressed throughout S-1, up to the position of the presumptive somite boundary (Fig. 3D). High-level Dll3 expression is therefore restricted to the PSM. In contrast, Notch1 was highest in the forming (S0) and nascent somites (S1) in the majority of embryos (Fig. 3E). In agreement with expression of the Notch1 mRNA (Fig. 3F) (20,55), high levels of Notch1 were not observed in somite S2 and beyond, and also decreased to background levels in more caudal regions of the PSM (Fig. 3E). Reciprocal expression patterns of Dll3 and Notch1 protein were evident in embryos, with significant co-expression of Dll3 and Notch1 restricted to a region of approximately one somite immediately caudal to the forming somite in S-1 (Fig. 3G). To determine whether vesicles containing Dll3 and Notch1 also harbour Dll1, we examined Dll1 expression in the rostral PSM. Dll1 and Notch1 exhibited some co-localization as Notch1 expression diminished caudally (Fig. 3H and I). We then examined Dll1, Dll3 and Notch1 simultaneously in the same embryo. Puncta positive for Notch1 and Dll3 were observed rostral to the border of Dll1 expression (Fig. 3J). Thus both Dll3 and Dll1 co-localize with Notch1 in the rostral PSM, although Dll3 co-localizes with Notch1 in more rostral regions where Dll3 expression persists. Cells undergoing Notch1 signalling can be identified with an antibody specific to the γ-secretase cleaved and hence active form of Notch1. Successive waves of Notch1 signalling emanate from the tail bud and propagate rostrally with a period of 120 min in the mouse, equal to the time taken to form a somite. In the rostral PSM, the wave slows and becomes restricted to a static band a few cells wide. It is at this point that the position of the next somite boundary is likely to be defined just caudal to the narrow band of cells undergoing Notch1 signalling (15,16). To determine where Notch1 signalling is actually occurring in relation to Dll3:Notch1 co-localization, we stained embryos for this γ-secretase-cleaved active Notch1 receptor. Dll3 and Notch1 co-localized in puncta between successive bands of Notch1 signalling or just rostral to the most rostral stripe of Notch1 signalling (Fig. 3K). Notch1/Dll3-positive puncta found in the rostral PSM (S-1) were excluded from the *cis*-Golgi as seen in embryos co-stained for anti-Dll3, anti-Notch1 and anti-GM130 (Fig. 3L). Thus, the expression level and subcellular localization of Dll3 differ between the caudal and rostral PSM. In the caudal PSM, Dll3 is highly expressed and is localized to the *cis*-Golgi, whereas in the rostral PSM (the region of S-1), Dll3 expression is downregulated and *cis*-Golgi localization is lost. In this region, residual Dll3 is limited to lysosomes that also contain Notch1. In summary, Dll3 and Notch1 have

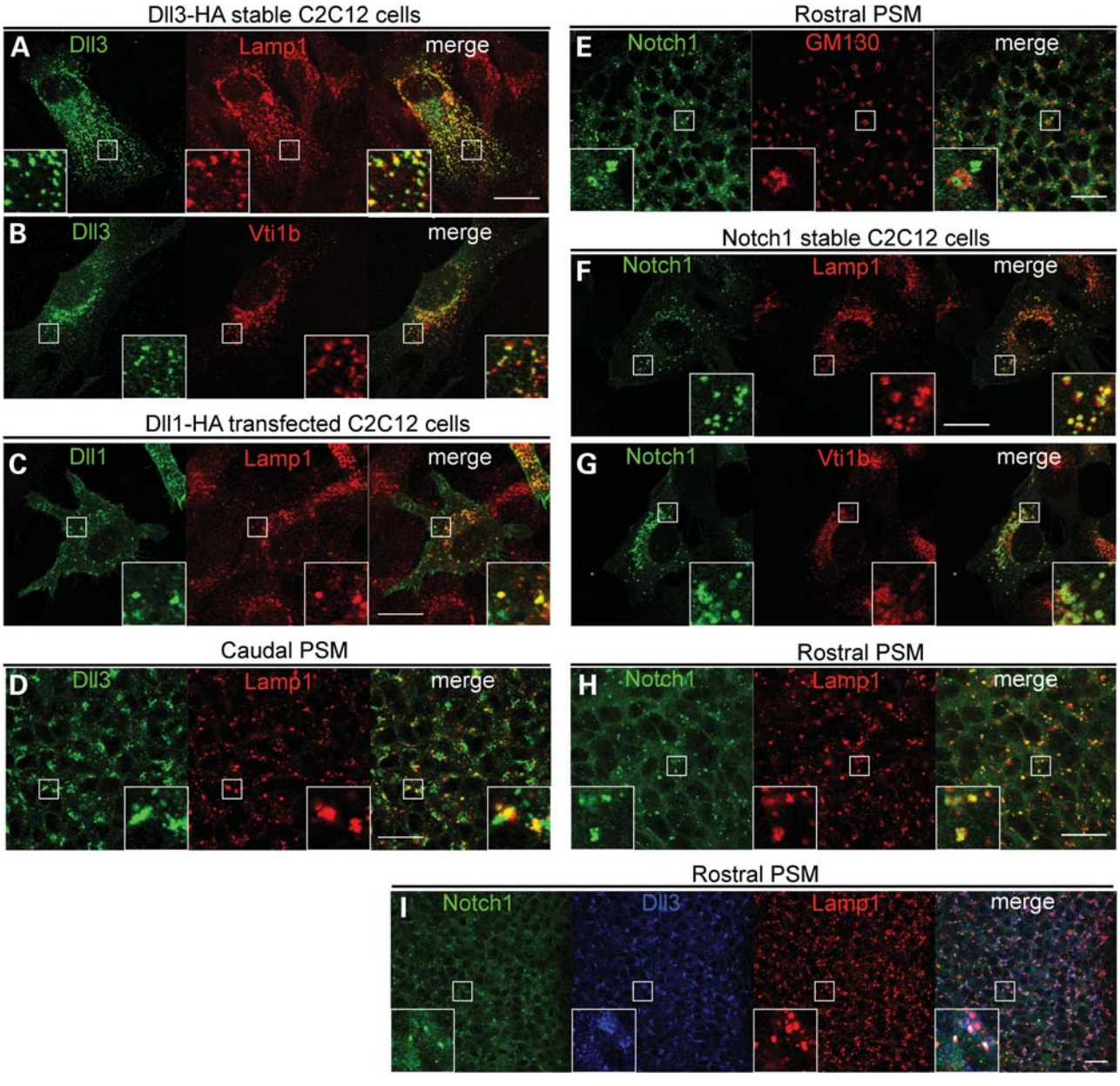

Figure 2. Notch1 and Dll3 localize to the late endocytic compartment. (**A**) Co-localization of Dll3 (αDll3, green) and Lamp1 (αLamp1, red) reactivity in C2C12 cells stably transfected with Dll3-HA. (**B**) Co-localization of Dll3 (αDll3, green) and Vti1b (αVti1b, red) reactivity in C2C12 cells stably transfected with Dll3-HA. The levels of the red channel have been adjusted. (**C**) Dll1 reactivity (αHA, green) is found in Lamp1-positive intracellular vesicles (αLamp1, red) in C2C12 transiently transfected with Dll1-HA. (**D**) Detection of Dll3 (αDll3, green) and Lamp1 (αLamp1, red) in the caudal PSM of a 9.5 dpc mouse embryo. (**E**) Rostral PSM from a 9.5 dpc embryo stained to detect Notch1 (αNotch1, green) and GM130 reactivity (αGM130, red). (**F**) Co-localization of Notch1 (αNotch1, green) and Lamp1 reactivity (αLamp1, red) in C2C12 cells stably expressing Notch1. (**G**) Detection of Notch1 (αNotch1, green) and Vti1b (αVti1b, red) reactivity in C2C12 cells stably expressing Notch1. (**H**) Co-localization of Notch1 (αNotch1, green) and Lamp1 (αLamp1, red) reactivity in the rostral PSM from a 9.5 dpc embryo. (**I**) Rostral PSM from a 9.5 dpc embryo stained to detect Notch1 (αNotch1, green), Dll3 (αDll3, blue) and Lamp1 reactivity (αLamp1, red). Scale bars represent 20 μm.

reciprocal expression domains that overlap in the rostral PSM (mainly S-1) between, and just rostral to, the static bands of Notch1 signalling (schematic summary in Fig. 4K, wild type).

Juxtaposition of Dll3 and Notch1 signalling supports an inhibitory role for Dll3 in the embryo

Signalling from the Notch1 receptor oscillates in the PSM (15,16). We compared Notch1 expression with Notch1 signalling in wild-type and *Dll3* null *(Dll3$^{neo/neo}$)* embryos. Activation of Notch1 signalling cycles in the PSM with the presence of successive waves (15,16). This results in domains of activated Notch1 in the PSM; in wild-type embryos, the narrowest domain is the most rostrally located (Fig. 4A, B and E; red). In contrast, *Dll3* null embryos lacked cyclic Notch1 activation in the caudal PSM and had only one broad rostral band of Notch1 signalling (Fig. 4C, D, I and J, red) (24). This band of Notch1 signalling failed

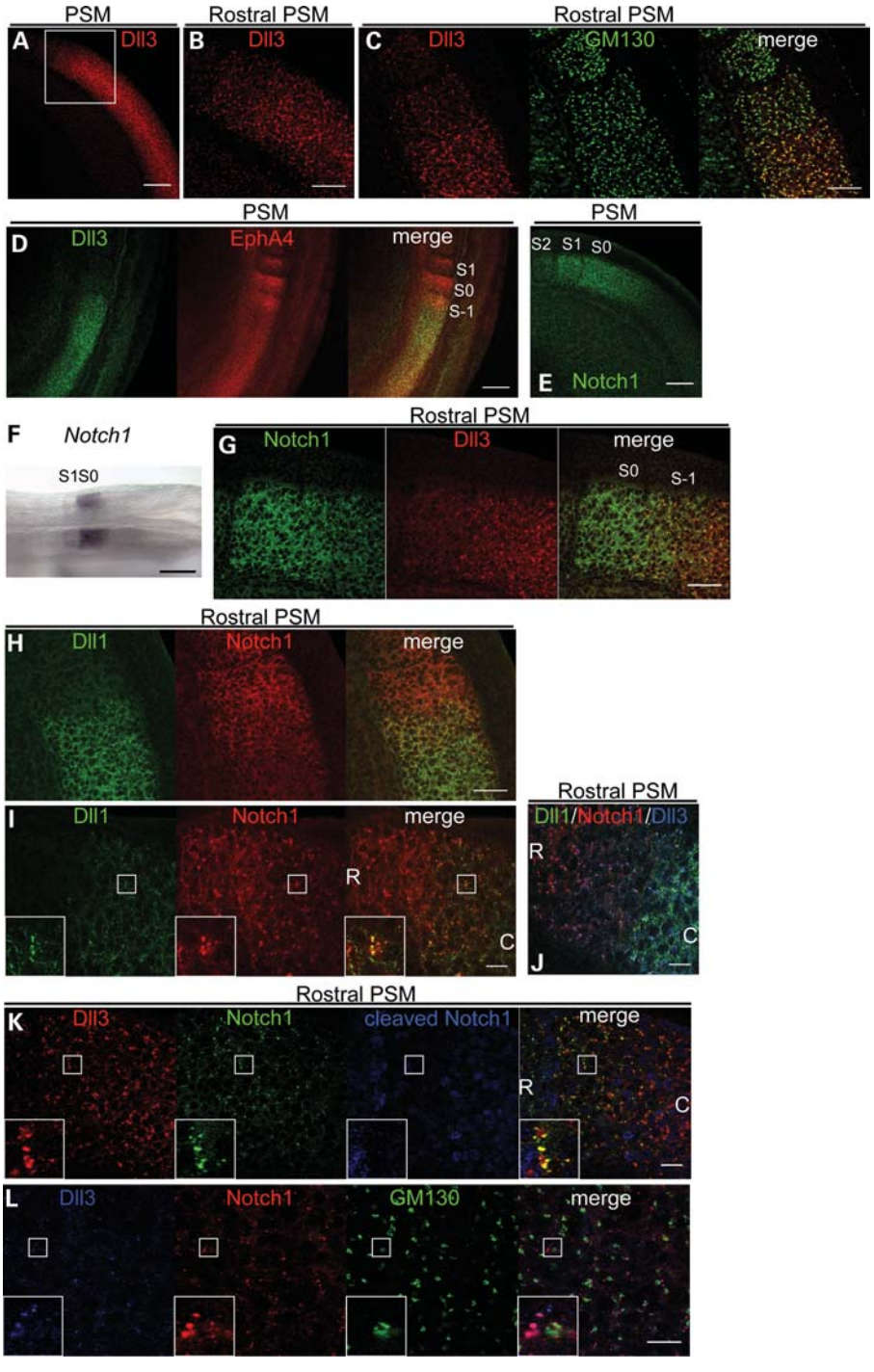

Figure 3. Dll3 and Notch1 have overlapping expression domains and co-localize in the rostral PSM. (**A**) Low (×16) and (**B**) high (×40) magnification of Dll3 reactivity (αDll3, red) in the PSM of a 9.5 dpc embryo. The square in (A) represents the magnified area shown in (B). (**C**) Wholemount immunofluorescence detection of Dll3 (αDll3, red) and GM130 (αGM130, green) reactivity in the rostral PSM at 9.5 dpc (**D**) Detection of Dll3 (αDll3, green) and EphA4 reactivity (αEphA4, red) in the PSM of a 9.5 dpc embryo. (**E**) Low power (×16) image of a 9.5 dpc embryo wholemount stained to detect Notch1 reactivity (αNotch1, green). (**F**) Wholemount RNA *in situ* hybridization detection of the Notch1 mRNA in a 9.5 dpc embryo. (**G**) Overlapping expression domains of Notch1 (αNotch1, green) and Dll3 (αDll3, red) in the rostral PSM of a 9.5 dpc embryo. (**H** and **I**) Wholemount immunofluorescence detection of Dll1 (αDll1, green) and Notch1 (αNotch1, red) reactivity in the rostral PSM of a 9.5 dpc embryo at ×40 (H) and ×63 (I) magnification. Co-localization of Notch1 and Dll1 appears yellow. (**J**) A high power (×63) image of the rostral PSM of a 9.5 dpc mouse embryo co-stained for Dll1 (αDll1, green), Notch1 (αNotch1, red) and Dll3 (αDll3, blue). Puncta positive for anti-Dll3 and anti-Notch1 reactivity appear violet. (**K**) Detection of Dll3 (αDll3, red), Notch1 (αNotch1, green) and cleaved Notch1 (α1744, blue) in the rostral PSM of a 9.5 dpc embryo. Puncta which contain anti-Dll3 and anti-Notch1 reactivity appear yellow. (**L**) Co-staining of the rostral PSM for Dll3 (αDll3, blue), Notch1 (αNotch1, red) and GM130 (αGM130, green). The last formed somite, the forming somite and the prospective somite are indicated as S1, S0 and S-1, respectively. Rostral (R)-to-caudal (C) orientation is indicated. Scale bars represent 200 μm in (F), 100 μm in (A), (D) and (E), 50 μm in (B), (C), (G) and (H) and 20 μm in (I–L).

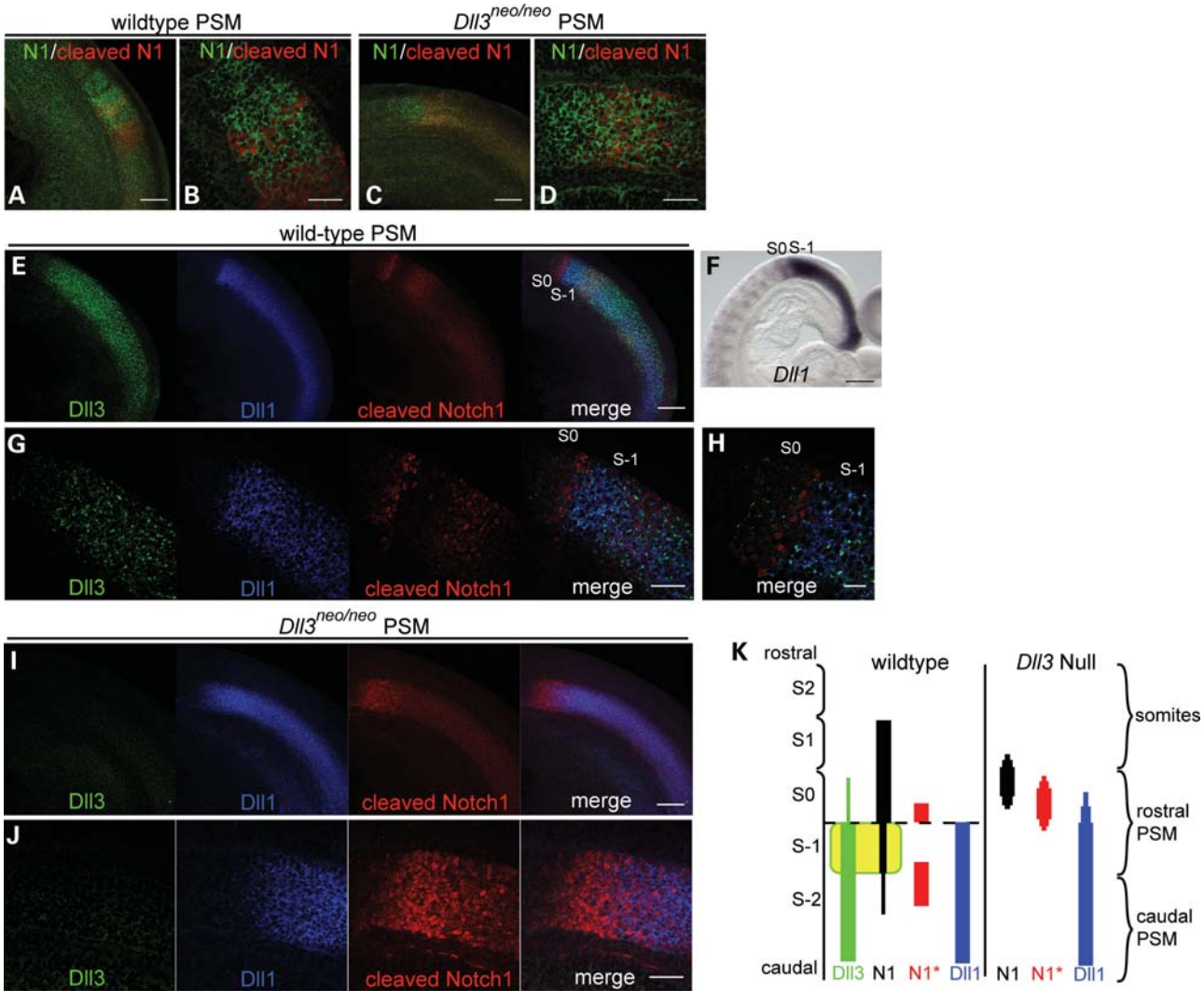

Figure 4. Detection of Notch1, Dll1, Dll3 and Notch1 signalling in wild-type and *Dll3* null PSM. (**A**–**D**) Detection of Notch1 (αNotch1, green) and cleaved Notch1 (α1744, red) reactivity by wholemount immunofluorescence in wild-type (A and B) and *Dll3* null 9.5 dpc embryos (C and D). (**E**, **G**–**J**) Wholemount immunofluorescence detection of Dll3 (αDll3, green), Dll1 (αDll1, blue) and cleaved Notch1 (α1744, red) in wild-type (E, G and H) and *Dll3* null 9.5 dpc embryos (I and J). (E) Low magnification (×16) of a wild-type embryo stained to detect anti-Dll3, anti-Dll1 and anti-cleaved Notch1. (**F**) Wholemount RNA *in situ* hybridization detection of the Dll1 mRNA in a 9.5 dpc embryo. (G) ×40 magnification of the rostral PSM of the embryo in (E). (H) ×63 magnification of the rostral PSM of the embryo in (E). (I) Low power (×16) of a *Dll3* null 9.5 dpc embryo stained to detect anti-Dll3, anti-Dll1 and anti-cleaved Notch1. (J) ×40 magnification of the *Dll3* null 9.5 dpc embryo in (I). The last formed somite, the forming somite and the prospective somite are indicated as S1, S0 and S-1, respectively. Scale bars represent 200 μm in (F), 100 μm in (A), (C), (E) and (I), 50 μm in (B), (D),(G) and (J) and 20 μm in (H). (**K**) A summary of Dll3 (green), Notch1 (black), cleaved Notch1(red) and Dll1 (blue) expression domains in the somites and PSM of wild-type and *Dll3* null 9.5 dpc embryos. The region of Dll3 and Notch1 co-localization is boxed in yellow.

to restrict to the thin stripe of cells observed in wild-type embryos (Fig. 4A–D). The expression of the Notch1 receptor overlapped with Notch1 signalling in wild-type and *Dll3* null embryos, but also extended more rostrally in both genotypes. To correlate Delta-like ligand expression with Notch1 signalling during somitogenesis, we examined Dll1, Dll3 and cleaved Notch1 in the same embryo. Dll1 protein was detected throughout the PSM (Fig. 4E, blue), consistent with the Dll1 mRNA (Fig. 4F) (56,57). However, Dll1 protein was not detected in the caudal half of each somite, in contrast to the transcript (Fig. 4E and F) (56). The rostral limit of Dll1 expression was abrupt and was directly adjacent to the most rostral stripe of Notch1 signalling (Fig. 4E, G and H; Supplementary Material, Fig. S3A and B). Dll1 expression in the PSM appeared stronger at its rostral limit, consistent with expression of the Dll1 mRNA (Fig. 4E and F). Rostral to this, Dll3 expression sharply decreased, although low-level expression continued for approximately one somite width (Fig. 4G and H; Supplementary Material, Fig. S3A and B, green). The situation is similar in 11.5 dpc embryos, although cyclic Notch1 activation was less obvious and the rostral stripe of Notch1 signalling was broader (Supplementary Material, Fig. S3C and D). In *Dll3* null 9.5 dpc embryos, Dll1 expression failed to sharpen at its rostral limit, instead a gradual taper of protein expression was detected in all *Dll3* null embryos examined (Fig. 4I and J, blue). Thus, there is a

correlation between a failure of rostral Dll1 expression to sharpen, and failure of Notch1 signalling to restrict to a thin stripe of cells in *Dll3* null embryos (Fig. 4I and J, red). The broad rostral domain of Notch1 signalling observed in all *Dll3* null embryos implies that this domain does not narrow and fade during the somitogenesis cycle as in wild type, but instead perpetuates through successive cycles. In conclusion, the rostro-caudal extent of Notch1, Dll1 and Dll3 expression in the PSM, and the inability of the Notch1 signalling domain to narrow in the rostral PSM in the absence of Dll3, indicates that Dll3 inhibits Notch1 signalling in the PSM of the embryo.

DISCUSSION

The pattern of Notch signalling in a given tissue is in part a product of the opposing functions of its ligands, as ligands can induce signalling *in trans* as well as inhibit signalling *in cis*. Induction of Notch signalling by ligand *in trans* is well studied, and the mechanism by which it occurs is largely defined (58). In stark contrast, the mechanism of *cis*-inhibition of Notch receptors by their ligands remains obscure. This may be because data addressing this issue have been generated using very different approaches; different classes of DSL ligand from different species have been examined using transgenesis in *Drosophila* or by overexpression in cultured mammalian cells (42–44). Moreover, many of the findings are likely to be confounded by the fact that the DSL ligands studied have both *trans*-activating as well as *cis*-inhibitory capabilities. We studied Dll3-mediated *cis*-inhibition, taking advantage of the fact that Dll3 is unique among Notch ligands because it acts solely to *cis*-inhibit Notch without the capacity to induce signalling *in trans* (44). In addition, we made use of cell lines expressing proteins at near-endogenous levels and verified our *in vitro* findings in the embryo. We demonstrate that Dll3 is not presented on the cell surface of PSM cells *in vivo*, consistent with our previous report that Dll3 is found in the Golgi apparatus (24). In addition, we also found Dll3 in late endosomes and lysosomes. This intracellular localization is consistent with the inability of Dll3 to induce signalling *in trans* (44) and implies that Dll3-mediated *cis*-inhibition occurs inside the cell. We also show that Dll3 interacts with the unprocessed full-length form of Notch1. Together, these findings place the interaction inside the cell because, first, Dll3 is localized inside the cell and, second, little or no full-length Notch1 is presented on the cell surface (27,28,52).

Defining the intracellular compartments in which Dll3 and Notch1 co-locate may infer the mechanism of inhibition. In C2C12 cells and *in vivo*, we found Notch1 in vesicles that also harbour the lysosomal marker Lamp1, placing it in lysosomes where it is presumably degraded. Lysosomal degradation of heterodimeric Notch1 has been previously reported (38). Full-length Notch1 is also likely to be lysosomal because Dll3 only interacts with full-length Notch1 and they co-localize to lysosomes. Notch1 has also been reported to co-localize with Hrs (multi-vesicular bodies) and Caveolin1 (caveolae) (39,59). However, we did not observe this in C2C12 cells. Instead, our findings are indicative of a late endosome/lysosome localization of Notch1. It is noteworthy that in the *Drosophila* eye, Notch does not co-localize with Hrs, but does with Rab7-EGFP, consistent with our findings (60). These data imply that Dll3 and Notch1 co-localize in late endosomes and degradative lysosomes. Taken together, our data indicate that Dll3 and full-length Notch1 interact inside the cell and co-localize to late endosome/lysosomes. Thus, Dll3 may alter the trafficking of full-length Notch1 by sequestering it to late endosome/lysosomes, thereby preventing its S1 processing. Once in the lysosomes, Dll3 may, in addition, cause the degradation of full-length Notch1; either of these possibilities would reduce cell surface levels of the receptor available for signalling. Ladi *et al.* (44) state that Dll3 expression does not reduce cell-surface Notch1; however, the transient overexpression of Notch1 in this case may have masked the function of Dll3. To circumvent this issue, we have attempted to quantify changes in cell surface presentation of endogenous Notch1, but have been unable to consistently detect endogenous Notch1 on the cell surface (data not shown).

The importance of identifying a mechanism for Dll3-mediated *cis*-inhibition of Notch1 signalling extends beyond Dll3 and somitogenesis. Other ligands of Notch (Dll1, Jag1, Dll4) also inhibit Notch signalling *in cis* (24,44; unpublished data). We believe that the mechanism of Dll3 *cis*-inhibition of Notch1 might also apply to *cis*-inhibition by other ligands for the following reasons: First, we show that transfected Dll1 co-precipitates more full-length Notch1 than heterodimeric Notch1, consistent with a previous report in the chick (42). Second, we demonstrate that Dll1 localizes to lysosomes in cultured cells. Establishing the mechanism of *cis*-inhibition of Notch for these other ligands will be complicated by the fact that they also interact with Notch *in trans*, further proving that the unique Dll3 ligand is singularly important in defining the mechanism of ligand-dependent *cis*-inhibition of Notch.

Dll3 function is central to somitogenesis in the mouse. In its absence, somite formation and patterning are irregular, leading to AVS, and in human causes the birth defect, SCD (1,22,61,62). Despite its importance, how Dll3 affects Notch1 signalling in the PSM during the dynamic and reiterative process of somitogenesis has remained elusive. A major impediment to this understanding stems from the fact that the study of somitogenesis has largely relied on the examination of transcript localization, but defining protein expression domains and subcellular localization is essential, especially in the control of Notch signalling, since it is expression of ligands and other proteins that determines the position and duration of Notch1 signalling during somitogenesis. We developed a wholemount immunofluorescence staining technique on mouse embryos (24) that we have used here to accurately map the cellular and subcellular localization of Dll3, Dll1 and Notch1 in the PSM during mouse somitogenesis. Using this approach, we have mapped the protein expression domains for Dll3, Dll1 and Notch1 and have established regions of subcellular co-localization. Superimposed on this, we have defined regions of cells undergoing Notch1 signalling and have shown that this is perturbed in the PSM of *Dll3* null mice (Fig. 4K). Aware of the complication imparted by the dynamic nature of ligand and receptor expression and

Notch1 signalling during the somitogenesis cycle, we draw the following conclusions: first, high levels of Dll3 and Notch1 expression appear mutually exclusive; Notch1 predominates in regions S1 and S0, whereas Dll3 predominates in S-2. We have additional evidence in support of this observation; exogenous expression of Dll3 and Notch1 is mutually exclusive in C2C12 cells (Supplementary Material, Fig. S3E and F). Mutual exclusivity suggests in some regions of the PSM that Dll3 and Notch1 each causes the degradation of the other. Others have noted similar mutual exclusion between ligand and receptor. For example, Notch knockdown reduced DeltaD degradation in zebrafish, although *cis* and *trans* effects are both likely at play (63). Mutual inactivation of the ligand and receptor is an important aspect of a recent model indicating that *cis*-inhibition provides a sensitive switch between signal sending and receiving states to aid Notch-dependent boundary formation and lateral inhibition events (64). Importantly, a region of mutual Dll3 (high) and Notch1 (medium) expression occurs in the region of S-1. It is here that these proteins co-localize in degradative lysosomes. Consequently, Notch1 is not available on the cell surface to be activated by Dll1 *in trans*, and accordingly we do not detect activated Notch1 in this S-1 region. Further proof to support the model for how Dll3 *cis*-inhibits Notch1 signalling would be that Dll3 reduces the level of Notch1 cell surface presentation. Nonetheless, our findings in the PSM of *Dll3* null mice support these conclusions, as in the absence of the *cis*-inhibitory ligand, the domain of activated Notch1 is extended in the S0 to S-1 region of the PSM.

MATERIALS AND METHODS

Plasmids

Mouse cDNAs of Dll1, Jagged1 and Dll3 were cloned into the expression vector pCMX (65) using the Gateway System (Invitrogen). Dll3 was Gateway-cloned into pCMX-HA and pCAG-HA-iPuro to create Dll3HApCMX and pCAG-Dll3HA-iPuro, respectively. pCAG-N1myc-iNeo was created by gateway-cloning Notch1myc into pCAGiNeo. HA-tagged Dll1 was generated by cloning an adaptor encoding the HA tag into the unique Mfe1 site of mouse Dll1.

Cell culture and generation of stable cell lines

C2C12 (ATCC) and HEK293 cells (Invitrogen) were grown in DMEM containing 10% FCS. A C2C12 line stably expressing myc-tagged Notch1 was described previously (66). pCAG-N1myc-iPuro (66) was used to generate HEK293 cells stably expressing Notch1. C2C12 cells stably overexpressing HA-tagged Dll3 were generated using pCAG-Dll3HA-iPuro. Notch1myc was introduced into Dll3HA-expressing C2C12 cells by stable transfection of pCAG-N1myc-iNeo. Stable lines were generated by selection in either 1.5 μg/ml puromycin or 250 μg/ml G418 for 10 days. Isolated cell clones were picked, expanded and analysed for protein expression by immunofluorescence and western blotting with anti-HA or anti-myc antibodies.

Immunofluorescence and imaging

Immunocytochemistry on fixed cells was performed as described previously (67). Immunocytochemistry on unfixed cells was performed as follows: transfected C2C12 cells on coverslips were chilled on ice for 20 min in cold growth media (DMEM containing 10% FCS). The media was replaced with primary antibody diluted in media and incubated on ice for 1 h. Cells were rinsed three times in cold media and then washed finally for 10 min in cold media prior to fixation for 15 min in cold 4% PFA dissolved in PBS containing 1 mM $MgCl_2$ and 0.1 mM $CaCl_2$. Additional primary and secondary antibody detection was performed as described previously (67), except that 1 mM $MgCl_2$ and 0.1 mM $CaCl_2$ were included in all solutions. Wholemount immunofluorescence on fixed embryos was performed as described in Geffers *et al*. (24). Wholemount immunofluorescence on fresh unfixed embryos was performed as follows. Mouse embryos (9.5 dpc) were dissected in M2 medium. The tail was dissected and then bissected down the neural tube. Embryos to be permeabilized were treated with 0.1% Triton in M2 on ice for 15 min and then washed twice in M2. Embryos were blocked in M2 on ice for 30 min prior to the addition of primary antibodies against the amino terminal peptides in Dll1 (1F9) and Dll3 (N2) (24). The following day, embryos were washed three times in cold M2 medium, fixed in cold 4% PFA for 15 min on ice, washed in 150 mM glycine in PBS for 15 min and then twice in M2 medium before the addition of the secondary antibodies. After 2 h, the embryos were washed twice in M2 medium, then once in PBS and flat-mounted in Prolong antifade reagent (Invitrogen). Fluorescence from Alexa 488 (Invitrogen), Dylight 488 (Jackson ImmunoResearch), Cy3 and Cy5 conjugates to donkey secondary antibodies (Jackson ImmunoResearch) and eGFP were collected using laser scanning confocal microscopes (Leica TCS SP upright and Zeiss 710 on an AxioObserver inverted Z1). Images are single sections generated using the manufacturer's software. Levels adjustment, carried using PhotoShop CS4 (Adobe) was uniform unless noted in the figure legend. Scale bars were added in ImageJ (NIH) and figures were assembled using Illustrator CS4 (Adobe).

Precipitation of cell-surface proteins, co-immunoprecipitation and western blotting

Cell-surface proteins were precipitated by the biotinylation method as described previously (52) with the following modifications. Transfected cells were grown to 80–90% confluency on 60 mm dishes, washed three times with ice-cold PBS containing 1 mM $MgCl_2$ and 0.1 mM $CaCl_2$ (PBS++) and then incubated with PBS++ containing 0.5 mg/ml NHS-sulfo-biotin (Pierce) for 2 h on ice. The biotin reagent was aspirated and quenched by the addition of cold DMEM for 10 min on ice. The cells were then washed three times in PBS++ and lysed in 0.5 ml of RIPA buffer [20 mM Tris, pH 7.5, 2 mM EDTA, 150 mM NaCl, 1% NP-40, 1% sodium deoxycholate, 0.1% SDS, EDTA-free Complete protease inhibitors (Roche) and 1 mM PMSF (Sigma)] for 30 min on ice. Each lysate was put through a 30 Gauge needle four times and centrifuged at 13 000 rpm for 15 min at 4°C. The supernatant was

collected and incubated with BSA-blocked streptavidin beads (Pierce) overnight at 4°C. The beads were washed three times in RIPA buffer and finally in cold 0.9% NaCl before the addition of LDS load buffer (Invitrogen). Samples were heated to 100°C for 10 min and loaded on Novex 3–8% Tris acetate gels and subjected to western blot analysis.

Co-immunoprecipitations were performed on transfected cells lysed in IP buffer [20 mM Hepes pH 7.5, 150 mM KCl, 2 mM EGTA, 1% CHAPS, EDTA-free Complete protease inhibitors and 1 mM PMSF]. Lysates were incubated with 1–3 μg of antibody at 4°C overnight and then with 50 μl of Protein G-beads (Amersham) for a further 2 h. The beads were washed three to four times with 500 μl of IP buffer, then mixed with LDS load buffer and heated to 70°C for 10 min. Samples were then loaded on Novex 3–8% Tris acetate gels and subjected to western blotting.

RNA *in situ* hybridization

Wholemount RNA *in situ* hybridization was performed as described previously (57). cDNA probes used were Notch1 (68) and Dll1 (56).

SUPPLEMENTARY MATERIAL

Supplementary Material is available at *HMG* online.

ACKNOWLEDGEMENTS

We would like to thank Achim Gossler for critical reading of the manuscript; Joelene Major, Kavitha Iyer, Wendy Chen-Nee Chua and Natalie Wise for technical assistance; Robert Bryson-Richardson and Owen Prall for advice; Harold Stenmark for anti-Hrs antibody; Susanne Pfeffer for Rab7-EGFP and Rab9-EGFP; David Wilkinson for anti-EphA4 antibody; and Herbert Smith for generously donating the confocal microscope used in this study.

Conflict of Interest statement. None declared.

FUNDING

This work was supported by the National Health and Medical Research Council (grant numbers 404804, 635500, 514900 to S.L.D.); Australian Research Council (grant number DP1094119); and the Cancer Institute of NSW (grant number 06/ECF/1-03 to G.C.).

REFERENCES

1. Bulman, M.P., Kusumi, K., Frayling, T.M., McKeown, C., Garrett, C., Lander, E.S., Krumlauf, R., Hattersley, A.T., Ellard, S. and Turnpenny, P.D. (2000) Mutations in the human delta homologue, DLL3, cause axial skeletal defects in spondylocostal dysostosis. *Nat. Genet.*, **24**, 438–441.
2. Whittock, N.V., Sparrow, D.B., Wouters, M.A., Sillence, D., Ellard, S., Dunwoodie, S.L. and Turnpenny, P.D. (2004) Mutated MESP2 causes spondylocostal dysostosis in humans. *Am. J. Hum. Genet.*, **74**, 1249–1254.
3. Sparrow, D.B., Chapman, G., Wouters, M.A., Whittock, N.V., Ellard, S., Fatkin, D., Turnpenny, P.D., Kusumi, K., Sillence, D. and Dunwoodie, S.L. (2006) Mutation of the LUNATIC FRINGE gene in humans causes spondylocostal dysostosis with a severe vertebral phenotype. *Am. J. Hum. Genet.*, **78**, 28–37.
4. Sparrow, D.B., Guillén-Navarro, E., Fatkin, D. and Dunwoodie, S.L. (2008) Mutation of Hairy-and-Enhancer-of-Split-7 in humans causes spondylocostal dysostosis. *Hum. Mol. Genet.*, **17**, 3761–3766.
5. Tam, P.P. (1981) The control of somitogenesis in mouse embryos. *J. Embryol. Exp. Morph.*, **65** (suppl.), 103–128.
6. O'Rahilly, R., Muller, F. and Meyer, D.B. (1980) The human vertebral column at the end of the embryonic period proper. 1. The column as a whole. *J. Anat.*, **131**, 565–575.
7. William, D.A., Saitta, B., Gibson, J.D., Traas, J., Markov, V., Gonzalez, D.M., Sewell, W., Anderson, D.M., Pratt, S.C., Rappaport, E.F. *et al.* (2007) Identification of oscillatory genes in somitogenesis from functional genomic analysis of a human mesenchymal stem cell model. *Dev. Biol.*, **305**, 172–186.
8. Sparrow, D.B., Chapman, G., Turnpenny, P.D. and Dunwoodie, S.L. (2007) Disruption of the somitic molecular clock causes abnormal vertebral segmentation. *Birth Defects Res. C. Embryo Today*, **81**, 93–110.
9. Dequéant, M.-L., Glynn, E., Gaudenz, K., Wahl, M., Chen, J., Mushegian, A. and Pourquié, O. (2006) A complex oscillating network of signaling genes underlies the mouse segmentation clock. *Science*, **314**, 1595–1598.
10. Niwa, Y., Masamizu, Y., Liu, T., Nakayama, R., Deng, C.X. and Kageyama, R. (2007) The initiation and propagation of Hes7 oscillation are cooperatively regulated by Fgf and notch signaling in the somite segmentation clock. *Dev. Cell*, **13**, 298–304.
11. Morales, A.V., Yasuda, Y. and Ish-Horowicz, D. (2002) Periodic Lunatic fringe expression is controlled during segmentation by a cyclic transcriptional enhancer responsive to notch signaling. *Dev. Cell*, **3**, 63–74.
12. Krebs, L.T., Deftos, M.L., Bevan, M.J. and Gridley, T. (2001) The Nrarp gene encodes an ankyrin-repeat protein that is transcriptionally regulated by the notch signaling pathway. *Dev. Biol.*, **238**, 110–119.
13. Jouve, C., Palmeirim, I., Henrique, D., Beckers, J., Gossler, A., Ish-Horowicz, D. and Pourquié, O. (2000) Notch signalling is required for cyclic expression of the hairy-like gene HES1 in the presomitic mesoderm. *Development*, **127**, 1421–1429.
14. Sewell, W., Sparrow, D.B., Smith, A.J., Gonzalez, D.M., Rappaport, E.F., Dunwoodie, S.L. and Kusumi, K. (2009) Cyclical expression of the Notch/Wnt regulator Nrarp requires modulation by Dll3 in somitogenesis. *Dev. Biol.*, **329**, 400–409.
15. Morimoto, M., Takahashi, Y., Endo, M. and Saga, Y. (2005) The Mesp2 transcription factor establishes segmental borders by suppressing Notch activity. *Nature*, **435**, 354–359.
16. Huppert, S.S., Ilagan, M.X., De Strooper, B. and Kopan, R. (2005) Analysis of Notch function in presomitic mesoderm suggests a gamma-secretase-independent role for presenilins in somite differentiation. *Dev. Cell*, **8**, 677–688.
17. Ozbudak, E.M. and Lewis, J. (2008) Notch signalling synchronizes the zebrafish segmentation clock but is not needed to create somite boundaries. *PLoS Genet.*, **4**, e15.
18. Feller, J., Schneider, A., Schuster-Gossler, K. and Gossler, A. (2008) Noncyclic Notch activity in the presomitic mesoderm demonstrates uncoupling of somite compartmentalization and boundary formation. *Genes Dev.*, **22**, 2166–2171.
19. Conlon, R.A., Reaume, A.G. and Rossant, J. (1995) Notch1 is required for the coordinate segmentation of somites. *Development*, **121**, 1533–1545.
20. Barrantes, I.B., Elia, A.J., Wünsch, K., Hrabe de Angelis, M.H., Mak, T.W., Rossant, J., Conlon, R.A., Gossler, A. and de la Pompa, J.L. (1999) Interaction between Notch signalling and Lunatic fringe during somite boundary formation in the mouse. *Curr. Biol.*, **9**, 470–480.
21. Jiang, Y.J., Aerne, B.L., Smithers, L., Haddon, C., Ish-Horowicz, D. and Lewis, J. (2000) Notch signalling and the synchronization of the somite segmentation clock. *Nature*, **408**, 475–479.
22. Dunwoodie, S.L., Clements, M., Sparrow, D.B., Sa, X., Conlon, R.A. and Beddington, R.S. (2002) Axial skeletal defects caused by mutation in the spondylocostal dysplasia/pudgy gene Dll3 are associated with disruption of the segmentation clock within the presomitic mesoderm. *Development*, **129**, 1795–1806.
23. Kusumi, K., Mimoto, M.S., Covello, K.L., Beddington, R.S., Krumlauf, R. and Dunwoodie, S.L. (2004) Dll3 pudgy mutation differentially disrupts dynamic expression of somite genes. *Genesis*, **39**, 115–121.

24. Geffers, I., Serth, K., Chapman, G., Jaekel, R., Schuster-Gossler, K., Cordes, R., Sparrow, D.B., Kremmer, E., Dunwoodie, S.L., Klein, T. *et al.* (2007) Divergent functions and distinct localization of the Notch ligands DLL1 and DLL3 *in vivo*. *J. Cell Biol.*, **178**, 465–476.
25. Luo, Y. and Haltiwanger, R.S. (2005) O-fucosylation of notch occurs in the endoplasmic reticulum. *J. Biol. Chem.*, **280**, 11289–11294.
26. Shi, S. and Stanley, P. (2003) Protein *O*-fucosyltransferase 1 is an essential component of Notch signaling pathways. *Proc. Natl Acad. Sci. USA*, **100**, 5234–5239.
27. Blaumueller, C.M., Qi, H., Zagouras, P. and Artavanis-Tsakonas, S. (1997) Intracellular cleavage of Notch leads to a heterodimeric receptor on the plasma membrane. *Cell*, **90**, 281–291.
28. Logeat, F., Bessia, C., Brou, C., LeBail, O., Jarriault, S., Seidah, N.G. and Israel, A. (1998) The Notch1 receptor is cleaved constitutively by a furin-like convertase. *Proc. Natl Acad. Sci. USA*, **95**, 8108–8112.
29. Moloney, D.J., Panin, V.M., Johnston, S.H., Chen, J., Shao, L., Wilson, R., Wang, Y., Stanley, P., Irvine, K.D., Haltiwanger, R.S. *et al.* (2000) Fringe is a glycosyltransferase that modifies Notch. *Nature*, **406**, 369–375.
30. Mumm, J.S., Schroeter, E.H., Saxena, M.T., Griesemer, A., Tian, X., Pan, D.J., Ray, W.J. and Kopan, R. (2000) A ligand-induced extracellular cleavage regulates gamma-secretase-like proteolytic activation of Notch1. *Mol. Cell*, **5**, 197–206.
31. Nichols, J.T., Miyamoto, A., Olsen, S.L., D'Souza, B., Yao, C. and Weinmaster, G. (2007) DSL ligand endocytosis physically dissociates Notch1 heterodimers before activating proteolysis can occur. *J. Cell Biol.*, **176**, 445–458.
32. De Strooper, B., Annaert, W., Cupers, P., Saftig, P., Craessaerts, K., Mumm, J.S., Schroeter, E.H., Schrijvers, V., Wolfe, M.S., Ray, W.J. *et al.* (1999) A presenilin-1-dependent gamma-secretase-like protease mediates release of Notch intracellular domain. *Nature*, **398**, 518–522.
33. Jarriault, S., Brou, C., Logeat, F., Schroeter, E.H., Kopan, R. and Israël, A. (1995) Signalling downstream of activated mammalian Notch. *Nature*, **377**, 355–358.
34. Schroeter, E.H., Kisslinger, J.A. and Kopan, R. (1998) Notch-1 signalling requires ligand-induced proteolytic release of intracellular domain. *Nature*, **393**, 382–386.
35. Wu, L., Aster, J.C., Blacklow, S.C., Lake, R., Artavanis-Tsakonas, S. and Griffin, J.D. (2000) MAML1, a human homologue of *Drosophila* mastermind, is a transcriptional co-activator for NOTCH receptors. *Nat. Genet.*, **26**, 484–489.
36. Kurooka, H. and Honjo, T. (2000) Functional interaction between the mouse notch1 intracellular region and histone acetyltransferases PCAF and GCN5. *J. Biol. Chem.*, **275**, 17211–17220.
37. Wallberg, A.E., Pedersen, K., Lendahl, U. and Roeder, R.G. (2002) p300 and PCAF act cooperatively to mediate transcriptional activation from chromatin templates by notch intracellular domains *in vitro*. *Mol. Cell. Biol.*, **22**, 7812–7819.
38. Jehn, B.M., Dittert, I., Beyer, S., von der Mark, K. and Bielke, W. (2002) c-Cbl binding and ubiquitin-dependent lysosomal degradation of membrane-associated Notch1. *J. Biol. Chem.*, **277**, 8033–8040.
39. McGill, M.A., Dho, S.E., Weinmaster, G. and McGlade, C.J. (2009) Numb regulates post-endocytic trafficking and degradation of notch1. *J. Biol. Chem.*, **284**, 26427–26438.
40. Chastagner, P., Israël, A. and Brou, C. (2008) AIP4/Itch regulates Notch receptor degradation in the absence of ligand. *PLoS One*, **3**, e2735.
41. van Meel, E. and Klumperman, J. (2008) Imaging and imagination: understanding the endo-lysosomal system. *Histochem. Cell Biol.*, **129**, 253–266.
42. Sakamoto, K., Ohara, O., Takagi, M., Takeda, S. and Katsube, K. (2002) Intracellular cell-autonomous association of Notch and its ligands: a novel mechanism of Notch signal modification. *Dev. Biol.*, **241**, 313–326.
43. Glittenberg, M., Pitsouli, C., Garvey, C., Delidakis, C. and Bray, S. (2006) Role of conserved intracellular motifs in Serrate signalling, cis-inhibition and endocytosis. *EMBO J.*, **25**, 4697–4706.
44. Ladi, E., Nichols, J.T., Ge, W., Miyamoto, A., Yao, C., Yang, L.T., Boulter, J., Sun, Y.E., Kintner, C. and Weinmaster, G. (2005) The divergent DSL ligand Dll3 does not activate Notch signaling but cell autonomously attenuates signaling induced by other DSL ligands. *J. Cell Biol.*, **170**, 983–992.
45. Pourquié, O. and Tam, P.P. (2001) A nomenclature for prospective somites and phases of cyclic gene expression in the presomitic mesoderm. *Dev. Cell*, **1**, 619–620.
46. D'souza, B., Miyamoto, A. and Weinmaster, G. (2008) The many facets of Notch ligands. *Oncogene*, **27**, 5148–5167.
47. Fiúza, U.-M. and Arias, A.M. (2007) Cell and molecular biology of Notch. *J. Endocrinol.*, **194**, 459–474.
48. Blau, H.M., Pavlath, G.K., Hardeman, E.C., Chiu, C.P., Silberstein, L., Webster, S.G., Miller, S.C. and Webster, C. (1985) Plasticity of the differentiated state. *Science*, **230**, 758–766.
49. Yaffe, D. and Saxel, O. (1977) Serial passaging and differentiation of myogenic cells isolated from dystrophic mouse muscle. *Nature*, **270**, 725–727.
50. Kopan, R., Nye, J.S. and Weintraub, H. (1994) The intracellular domain of mouse Notch: a constitutively activated repressor of myogenesis directed at the basic helix–loop–helix region of MyoD. *Development*, **120**, 2385–2396.
51. Kuroda, K., Tani, S., Tamura, K., Minoguchi, S., Kurooka, H. and Honjo, T. (1999) Delta-induced Notch signaling mediated by RBP-J inhibits MyoD expression and myogenesis. *J. Biol. Chem.*, **274**, 7238–7244.
52. Bush, G., diSibio, G., Miyamoto, A., Denault, J.B., Leduc, R. and Weinmaster, G. (2001) Ligand-induced signaling in the absence of furin processing of Notch1. *Dev. Biol.*, **229**, 494–502.
53. Gordon, W.R., Vardar-Ulu, D., L'heureux, S., Ashworth, T., Malecki, M.J., Sanchez-Irizarry, C., Mcarthur, D.G., Histen, G., Mitchell, J.L., Aster, J.C. *et al.* (2009) Effects of S1 cleavage on the structure, surface export, and signaling activity of human Notch1 and Notch2. *PLoS One*, **4**, e6613.
54. Irving, C., Nieto, M.A., DasGupta, R., Charnay, P. and Wilkinson, D.G. (1996) Progressive spatial restriction of Sek-1 and Krox-20 gene expression during hindbrain segmentation. *Dev. Biol.*, **173**, 26–38.
55. Swiatek, P.J., Lindsell, C.E., del Amo, F.F., Weinmaster, G. and Gridley, T. (1994) Notch1 is essential for postimplantation development in mice. *Genes Dev.*, **8**, 707–719.
56. Bettenhausen, B., Hrabé de Angelis, M., Simon, D., Guénet, J.L. and Gossler, A. (1995) Transient and restricted expression during mouse embryogenesis of Dll1, a murine gene closely related to *Drosophila* Delta. *Development*, **121**, 2407–2418.
57. Dunwoodie, S.L., Henrique, D., Harrison, S.M. and Beddington, R.S. (1997) Mouse Dll3: a novel divergent Delta gene which may complement the function of other Delta homologues during early pattern formation in the mouse embryo. *Development*, **124**, 3065–3076.
58. Bray, S.J. (2006) Notch signalling: a simple pathway becomes complex. *Nat. Rev. Mol. Cell Biol.*, **7**, 678–689.
59. Okamura, Y. and Saga, Y. (2008) Pofut1 is required for the proper localization of the Notch receptor during mouse development. *Mech. Dev.*, **125**, 663–673.
60. Weber, U., Eroglu, C. and Mlodzik, M. (2003) Phospholipid membrane composition affects EGF receptor and Notch signaling through effects on endocytosis during *Drosophila* development. *Dev. Cell*, **5**, 559–570.
61. Kusumi, K., Sun, E.S., Kerrebrock, A.W., Bronson, R.T., Chi, D.C., Bulotsky, M.S., Spencer, J.B., Birren, B.W., Frankel, W.N. and Lander, E.S. (1998) The mouse pudgy mutation disrupts Delta homologue Dll3 and initiation of early somite boundaries. *Nat. Genet.*, **19**, 274–278.
62. Dunwoodie, S.L. (2009) The role of Notch in patterning the human vertebral column. *Curr. Opin. Genet. Dev.*, **19**, 329–337.
63. Matsuda, M. and Chitnis, A.B. (2009) Interaction with Notch determines endocytosis of specific Delta ligands in zebrafish neural tissue. *Development*, **136**, 197–206.
64. Sprinzak, D., Lakhanpal, A., Lebon, L., Santat, L.A., Fontes, M.E., Anderson, G.A., Garcia-Ojalvo, J. and Elowitz, M.B. (2010) Cis-interactions between Notch and Delta generate mutually exclusive signalling states. *Nature*, **465**, 86–90.
65. Umesono, K., Murakami, K.K., Thompson, C.C. and Evans, R.M. (1991) Direct repeats as selective response elements for the thyroid hormone, retinoic acid, and vitamin D3 receptors. *Cell*, **65**, 1255–1266.
66. Chapman, G., Liu, L., Sahlgren, C., Dahlqvist, C. and Lendahl, U. (2006) High levels of Notch signaling down-regulate Numb and Numblike. *J. Cell Biol.*, **175**, 535–540.
67. Dahlqvist, C., Blokzijl, A., Chapman, G., Falk, A., Dannaeus, K., Ibâñez, C.F. and Lendahl, U. (2003) Functional Notch signaling is required for BMP4-induced inhibition of myogenic differentiation. *Development*, **130**, 6089–6099.
68. Reaume, A.G., Conlon, R.A., Zirngibl, R., Yamaguchi, T.P. and Rossant, J. (1992) Expression analysis of a Notch homologue in the mouse embryo. *Dev. Biol.*, **154**, 377–387.